Impedance Shaping Controller for Robotic Applications in Interaction with Compliant Environments

Loris Roveda[1,2], Federico Vicentini[1], Nicola Pedrocchi[1], Francesco Braghin[2] and Lorenzo Molinari Tosatti[1]

[1]*Institute of Industrial Technologies and Automation (ITIA) of Italian National Research Council (CNR), via Bassini, 15 - 20133 Milan, Italy*

[2]*Politecnico di Milano, Department of Mechanical Engineering, via La Masa 1, 20156 Milan, Italy*

loris.roveda@itia.cnr.it

Keywords: Variable Impedance Control, Force-tracking Impedance Controls, Interacting Robotics Applications, Compliant Environments.

Abstract: The impedance shaping control is presented in this paper, providing an extension of standard impedance controller. The method has been conceived to avoid force overshoots in applications where there is the need to track a force reference. Force tracking performance are obtained tuning on-line both the position set-point and the stiffness and damping parameters, based on the force error and on the estimated stiffness of the interacting environment (an Extended Kalman Filter is used). The stability of the presented strategy has been studied through Lyapunov. To validate the performance of the control an assembly task is taken into account, considering the geometrical and mechanical properties of the environment (partially) unknown. Results are compared with constant stiffness and damping impedance controllers, which show force overshoots and instabilities.

1 INTRODUCTION

Robot machining and manipulation tasks require the control of the interaction between the robot and the surrounding environment, regardless the incompleteness and/or inaccuracies in the knowledge of the stiffness and location of the environment. In particular, compliant environments, *e.g.* in surgical applications, or high-added value materials could require a precise control of critical interaction forces during a task execution, *e.g.* avoiding force overshoots.

Principal methods for accomplishing robust and safe interactions certainly involve compliance controls. Since the milestones of sensor-based force/dynamics control (Salisbury, 1980; Mason, 1981; Raibert and Craig, 1981; Yoshikawa, 1987; Khatib, 1987; Yoshikawa and Sudou, 1990), dynamic balance between controlled robots and environments have primarily followed the approach of impedance controls (Hogan, 1984), including also non-restrictive assumptions (Colgate and Hogan, 1989) on the dynamical properties of the environment.

Impedance methods are proved to be dynamically equivalent to explicit force controls (Volpe and Khosla, 1995), but a direct tracking of explicit interaction forces or deformation is not straightforwardly allowed. To overcome this limitation, preserving the properties of impedance control, two different fami-

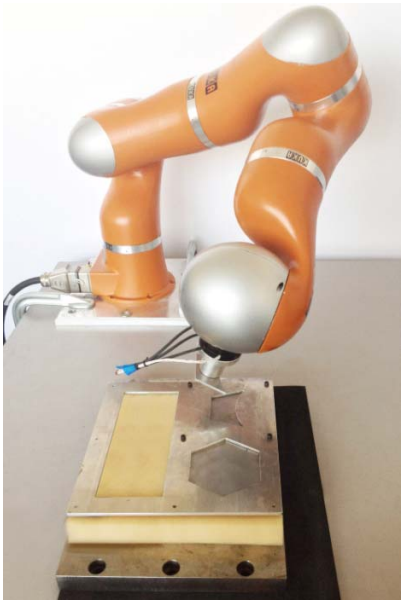

Figure 1: Experimental set-up for the assembly task execution.

lies of methods have been mainly introduced: (a) set-point deformation and (b) variable impedance adaptation.

For class (a), the most straightforward solution is suggested in (Villani et al., 1999), where the time-varying controlled force is derived from a position control law, scaling the trajectory as a function of the estimated environment stiffness. Another important approach (Seraji and Colbaugh, 1997) involves the generation of a reference motion as a function of the force-tracking error, under the condition that the environment stiffness is variously unknown, *i.e.* estimated as a function of the measured force. Commonly in (a), all approaches mantain a constant dynamic behaviour of the controlled robot, so that when the environment stiffness quickly and significantly changes, the bandiwth of the controllers has to be limited for avoiding instability.

Class (b) methods introduce the modification of the dynamic behaviour (*i.e.* online modification of the impedance parameters) during the task execution. Common solutions consist on gain/scheduling strategies that select the stiffness and damping parameters from a predefined set (off-line calculated) on the basis of the current target state (Ikeura and Inooka, 1995; Ferraguti et al., 2013). Such approaches are used in tasks characterized by a stationary, known and structured environment. When the environment is unknown or time-varying, the continuous adaptation of the impedance parameters out of a tracking error ensures better perfomance (Dubey et al., 1997; Park and Cho, 1998; Lee and Buss, 2000; Yang et al., 2011). To the best of authors' knowledge, no contributions are given to the impedance adaptation taking into account the runtime estimation of the environment stiffness. Remarkably, the discussed classes of algorithms are rarely applied in tasks where the environment properties change.

As a result, the main limitation in state-of-the-art methods is in terms of reduced bandwidth (*i.e.* limiting high perfomances) when the robot has to work (*e.g.* to machine, assemble, etc) in contact to unstructured and variable environments. Nevertheless, there is a wide range of interacting robotic applications (Roveda et al., 2013) in which it is important to estimate the environment dynamic parameters in order to improve the controller performances.

The purpose of the presented work is to extend the deformation/force-tracking impedance control to a global impedance *shaping*. This class (b) strategy introduces the ability to tune all impendance parameters (velocity/position set-point, stiffness and damping) at runtime, using both the tracking error and the estimate of the environment dynamic parameters. Equivalently, the impedance of the *global* system controlled robot-interacting environment is shaped to the task (unforeseen) properties.

The goals of such defined control strategy are to i) avoid force orvershoots that may damage the interacting environment ii) in applications where there is the need to track a force reference, iii) allowing maximum dynamic performance of the controlled robot. In adapting the parameters, for instance, stiffness and damping are defined as quadratic functions of the force error. This choice allows the definition of both high stiffness and low damping in the free space (in order to have maximum performances of the controlled robot to reach the target force reference) and low stiffness and high damping during contacts (in order to avoid force overshoots and to fit the dynamics of the environment), satisfying Lyapunov stability requirements.

The estimation of the environment stiffness is carried out by implementing an Extended Kalman Filter (EKF) as in (Roveda et al., 2013). The dynamic model of the interaction is based on a pure impedance model for both the controlled robot and the interacting compliant environment.

The effectiveness of the proposed control scheme is tested using a KUKA LWR 4+ manipulator in an assembly task (Figure 1). The task has been performed without knowing the environment's geometrical and mechanical properties. An assembly task has been selected due to its high relevance in industrial contexts.

2 PROBLEM FORMULATION AND CONTROL MODEL

Based on the estimate of the environment dynamic parameters and the force error $\mathbf{e}_f = \mathbf{f}^d - \mathbf{f_r}$, where $\mathbf{f}^d$ and $\mathbf{f_r}$ are the desired and measured robot forces, respectively, the impedance shaping control (Fig. 2) defines the set-point $\Delta\mathbf{x}_0$ and the stiffness and damping matrices $\mathbf{K},\mathbf{D}$ of the robot impedance control in order to shape the global impedance. A proportional term is used in order to track the desired interacting force. Stiffness and damping matrices are defined as a quadratic function of the force error. Symbolically

$$\mathbf{K} = \mathbf{K}_0 + \mathbf{m}_K \mathbf{e}_f^2 \tag{1}$$

$$\mathbf{D} = \mathbf{D}_0 + \mathbf{m}_D \mathbf{e}_f^2 \tag{2}$$

$$\Delta\mathbf{x}^0 = \mathbf{x} + \mathbf{K}_P \widehat{\mathbf{K}}_e^{-1} \mathbf{e}_f \tag{3}$$

$$\widehat{\mathbf{K}}_e = f(\mathbf{f}_e, \mathbf{x}_e^{eq}, \mathbf{x_e}) \tag{4}$$

where $\mathbf{K}$ is the diagonal stiffness matrix of the controlled robot, $\mathbf{K}_0$ is the diagonal stiffness matrix of

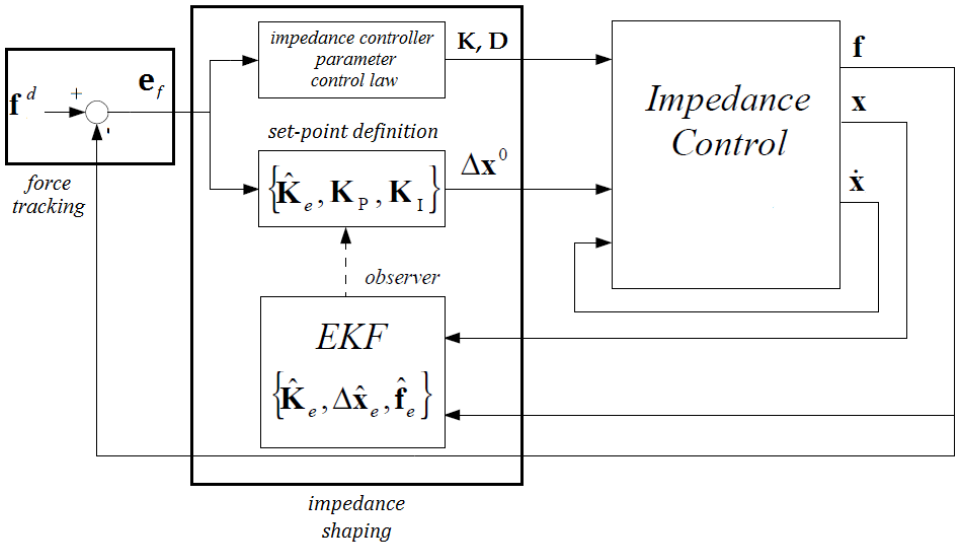

Figure 2: Impedance shaping control scheme: the set-point $\Delta\mathbf{x}_0$ and the stiffness and damping matrices $\mathbf{K},\mathbf{D}$ of the impedance control are defined. An EKF is implemented to estimate the environment stiffness used in the control law.

the controlled robot at zero-force error, $\mathbf{m}_K$ is the coefficient describing the quadratic function of the stiffness matrix with respect to the force error, $\mathbf{D}$ is the diagonal damping matrix of the impedance controller, $\mathbf{D}_0$ is the diagonal damping matrix of the impedance controller at zero-force error, $\mathbf{m}_D$ is the coefficient describing the quadratic function of the damping matrix with respect to the force error, $\mathbf{K}_P$ is the proportional gain, $\mathbf{f}_e$ is the force vector acting on the environment, $\mathbf{x}_e$ is the actual position of the environment and $\mathbf{x}_e^{eq}$ is the equilibrium position of the environment.

$\mathbf{K}_0$ is set equal to 100 $[N/m]$ and $\mathbf{D}_0$ is set to have an adimensional damping equal to 0.9 in order to have a high compliant behavior and high damping of the controlled robot with $\mathbf{f}_e = 0$, while $\mathbf{m}_K > 0$ and $\mathbf{m}_D < 0$ allow higher stiffness and smaller damping of the controlled robot in order to have higher performances with $\mathbf{f}_e \neq 0$.

The main task space impedance loop is performed by the model-based control of the manipulator at a rate of $200\,Hz$, synchronously with the environment estimation (*observer* in Figure 2). A model of the multi-port robot-environment interaction is needed to define the force setpoints in (3) through the environemt stiffness $\widehat{\mathbf{K}}_e$, which in turn is estimated through the deformation of the environment and the full state of robot kinematics and exchanged forces. Interaction states and parameters are eventually observed by an EKF as described in (Roveda et al., 2013). Signals in (1), (2) and (3) are updated to the main KUKA LWR control loop, whose remote control mode allows the tuning of all impedance parameters, together with the sampling of force and kinematics state. The remote controller is based on a real-time Linux Xenomai platform with RTNet-patched network interfaces.

3 COUPLED SYSTEM DYNAMICS

The dynamics of the coupled system, discussed for stability in Section 3.2, involve a balance between the environment and the control expressed through the exchanged forces (described in Section 3.1).

3.1 Impedance Control and Environment Model

As described in (Roveda et al., 2013), the dynamic behavior of the controlled robot is equivalent to a pure impedance system, where the stiffness $\mathbf{K}$ and the damping $\mathbf{D}$ matrices are diagonal:

$$\mathbf{D}\dot{\mathbf{x}} + \mathbf{K}\Delta\mathbf{x} = \mathbf{f}_r \tag{5}$$

where $\Delta\mathbf{x} = \mathbf{x} - \Delta\mathbf{x}^0$ is the difference between the actual robot pose and the desired one $\Delta\mathbf{x}^0$ as generated in (3) and $\mathbf{f}_r$ is the external interacting force/torque vector.

Moreover, the simplest way to describe the interacting environment is the linear KelvinVoigt contact model (Flügge, 1975), considering a pure impedance behavior of the interacting environment (mass $\mathbf{M}_e$ - spring $\mathbf{K}_e$ - damper $\mathbf{D}_e$ model):

$$\sum_i (\mathbf{M}_e^i \ddot{\mathbf{x}}_e^i + \mathbf{D}_e^i \dot{\mathbf{x}}_e^i + \mathbf{K}_e^i \Delta\mathbf{x}_e^i) = \mathbf{f}_e, \forall i = 1,\cdot,N \tag{6}$$

for all the finite number N of interaction ports.

Under the hypotehsis that exchanged forces at interaction ports remain unaltered by the port $\mathbf{f}_e = \mathbf{f}_r = \mathbf{f}$ in (3), (4), (5) and (6).

3.2 Closed-loop Dynamics and Stability

Considering a single stable contact point, *i.e.* $\mathbf{x}_e = \mathbf{x}$, with $\mathbf{x}_e^{eq} = 0$, and considering a single DoF (the impedance control decouples the DoFs of the controlled robot), the coupled dynamics is therefore defined using the Lagrangian approach:

$$\begin{cases} T = \frac{1}{2} M_e \dot{x}^2 \\ V = \frac{1}{2} K_e x^2 + \int K(e_f)(x - \Delta x^0)\delta x \\ D = \frac{1}{2} D_e \dot{x}^2 + \frac{1}{2} D(\dot{x} - \Delta \dot{x}^0)^2 \end{cases} \tag{7}$$

where T is the kinetic energy, V the potential energy and D the dissipative energy of the coupled system. Substituting 1, 2, 3 in 7 the potential energy becomes:

$$V = \frac{1}{2} K_e x^2 + \int (K_0 + m_K e_f^2)(-K_P K_e^{-1} e_f)\delta x \tag{8}$$

The dissipative energy becomes:

$$D = \frac{1}{2} D_e \dot{x}^2 + \frac{1}{2}(D_0 + m_D e_f^2)(-K_P K_e^{-1} \dot{e}_f)^2 \tag{9}$$

In order to study the coupled system stability, the kinetic, potential and dissipative energies have to be written only using state variables. Therefore, the force error $\mathbf{e}_f$ can be written as follow:

$$e_f = f^d - K_e x \tag{10}$$

Substituting 10 and by applying Lagrangian approach the dynamics of the coupled system results:

$$\begin{aligned} M_e \ddot{x} = &- \left[D_e + D_0 K_P^2\right] \dot{x} \\ &- m_D (f^d - K_e x)^2 K_P^2 \dot{x} - K_e x \\ &- \left[K_0 + m_K \left(f^d - K_e x\right)^2\right] (K_P x - K_P K_e^{-1} f^d) \end{aligned} \tag{11}$$

In order to analyze the stability of the closed-loop system, the positive scalar Lyapunov function candidate is defined as:

$$V_{Ly} = T + V \tag{12}$$

The Lyapunov function candidate is therefore defined as:

$$\begin{aligned} V_{Ly} = &\frac{1}{2} M_e \dot{x}^2 + \frac{1}{2} K_e x^2 \\ &+ \int K(x)(K_P x - K_P K_e^{-1} f^d)\delta x \end{aligned} \tag{13}$$

Having $\frac{1}{2} M_e \dot{x}^2 + \frac{1}{2} K_e x^2 \geq 0 \; \forall \; (x, \dot{x})$, only the integral needs to be verified:

$$\int K(x)(K_P x - K_P K_e^{-1} f^d)\delta x \geq 0 \tag{14}$$

Proof. Equation (13) can be written as follow:

$$\frac{\int K(x) x \delta x}{\int K(x) \delta x} \geq \frac{f^d}{K_e} \tag{15}$$

where the left side term is the baricenter of the function $K(x)$.

Based on the quadratic function $K(x) = ax^2 + bx + c$ defined in (1), the x-coordinate of its baricenter is:

$$\frac{-b}{2a} = \frac{f^d}{K_e} \tag{16}$$

so that, substituting (16) in (15), the condition in (15) becomes

$$\frac{f^d}{K_e} \geq \frac{f^d}{K_e}, \forall (x, \dot{x}) \tag{17}$$

■

On the other hand, the time differentiation of (12) gives:

$$\dot{V}_{Ly} = M_e \dot{x}\ddot{x} + K_e x \dot{x} + K(x)(K_P x - K_P K_e^{-1} f^d)\dot{x} \tag{18}$$

Substituting (11) in (18), results:

$$\begin{aligned} \dot{V}_{Ly} = &- \left[D_e + D_0 K_P^2\right] \dot{x}^2 \\ &- m_D (f^d - x K_e)^2 K_P^2 \dot{x}^2 \end{aligned} \tag{19}$$

With $m_D < 0$ and $\overline{m}_D$ defined as:

$$\overline{m}_D = -m_D \tag{20}$$

and imposing $\dot{V}_{Ly} < 0$, the Lyapunov conditions is:

$$(f^d - x K_e)^2 < \frac{D_0}{\overline{m}_D} + \frac{D_e}{\overline{m}_D K_P^2} \tag{21}$$

The closed-loop system is therefore asymptotically stable if the quadratic force error is bounded by the right side term of (21) . The damping quadratic function is built in order to maximize the damping term D_0. Moreover, it is possible to define the force reference in a way that bound the quadratic force error and ensure the closed-loop system stability.

4 EXPERIMENTAL TEST

The developed control strategy has been tested in an assembly task. The set-up of the experiment is shown in Figure 1. The experimental set-up includes a lightweight manipulator (KUKA LWR 4+) mounted on a rigid base and an interacting environment with two different stiffness levels, in order to test the control strategy with different environment's properties. In particular, the stiffness in the vertical direction Z is set to be soft (5000 $[N/m]$), while the stiffnesses in the X and Y directions are set to be stiff (20000 $[N/m]$). The impedance shaping control has been compared with 4 different constant impedance controllers in order to show its better behavior when tracking a force reference, using the same proportional and integral gains. In particular, for the constant impedance controllers the used stiffness and damping parameters are shown in Table 1.

In order to improve performances of the controller an integral term is considered in the set-point $\Delta\mathbf{x}^0$ definition:

$$\Delta\mathbf{x}^0 = \mathbf{K}_P\widehat{\mathbf{K}}_e^{-1}\mathbf{e}_f + \mathbf{K}_i\widehat{\mathbf{K}}_e^{-1}\int \mathbf{e}_f \qquad (22)$$

4.1 Force-Tracking in Assembly Task

The assembly task (see (Roveda et al., 2013) for discussion) is performed in 5 major phases:
Phase A: Approach and contact detection in the vertical direction Z.
Phase B: The on-line estimation of $\widehat{\mathbf{K}}_e$ in the vertical direction Z starts.
Phase C: Exploration along translation components and on-line estimation of $\widehat{\mathbf{K}}_e$. The impedance control set-point $\Delta\mathbf{x}^0$ and the controlled robot stiffness $\mathbf{K}$ and damping $\mathbf{D}$ are computed as a function of force-tracking error $\mathbf{e}_f = \mathbf{f}_{task}^d - \mathbf{f}$ (rotational components of

Table 1: The stiffness and damping parameters used in the selected application are shown. The constant impedance controllers parameters has been selected in order to test the impedance control with a soft and stiff behavior and with high and low damping.

Impedance Control Parameters		
	$Stiffness[N/m]$	$AdimensionalDamping$
A	shaped	shaped
B	5000	0.1
C	5000	0.9
D	1000	0.1
E	1000	0.9

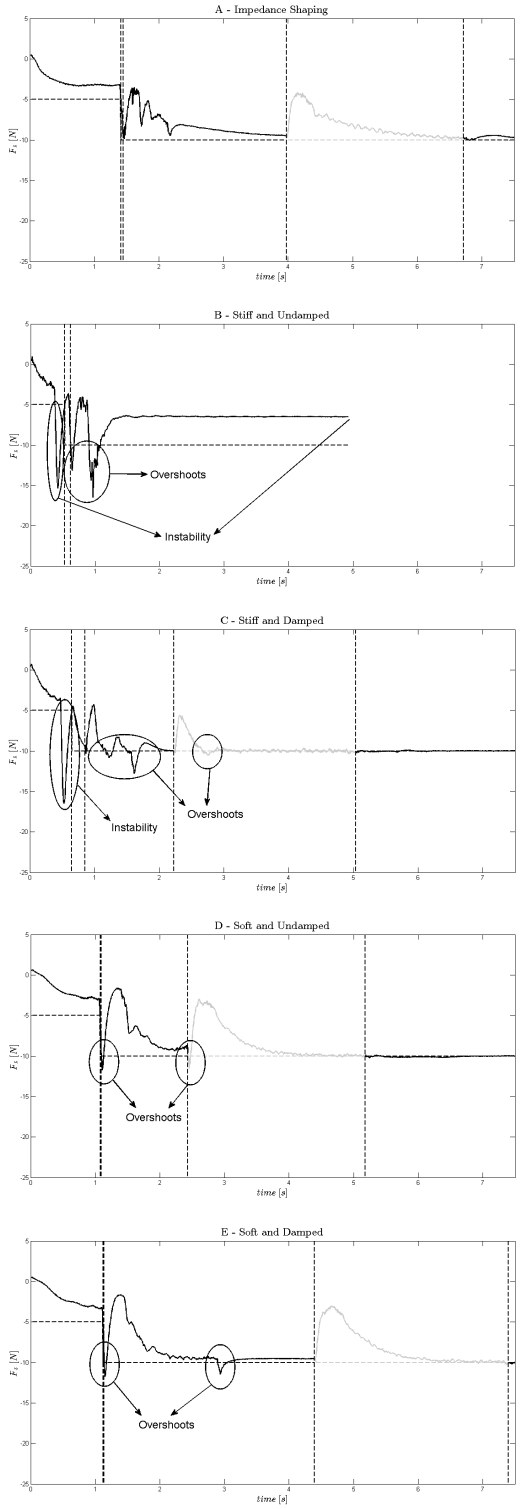

Figure 3: Desired forces (continuous lines) and measured forces (dashed lines) in direction Z during the assembly task for each control strategy. Phase *C* is highlighted in grey.

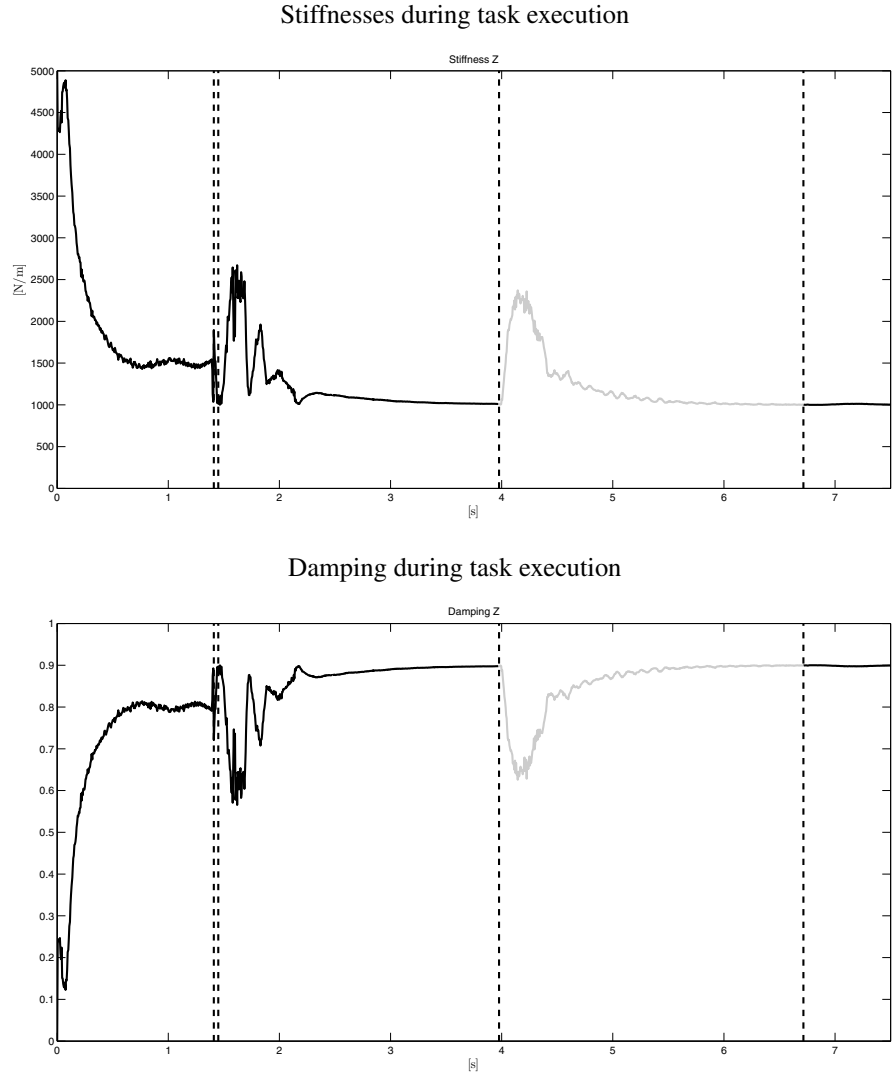

Figure 4: Impedance shaping control stiffness and damping parameters in direction Z during assembly task execution.

$\Delta\mathbf{x}^0$ are blocked).

Phase D: Assembly proper, enabling rotations for insertion and relying on $\widehat{\mathbf{K}}_e$ observed along the searching directions. The set-point $\mathbf{f}^d$ enables also torques.

Phase E: After tight assembly, on-line estimation of (possibly changing) $\widehat{\mathbf{K}}_e$.

Rotations in phase D are fastly executed to evaluate the capability of the control strategy to compensate force overshoots using constant rotational stiffness (100 [Nm/rad]) and damping parameters (0.9). In Figure 3 the measured interaction force in direction Z is shown, highlighting different phases. Experimental results show the capability of the impedance shaping control to avoid force overshoots even during phase D. Constant impedance controllers show force overshoots even using high damping and a very compliant behavior of the controlled robot. Constant high stiffness and low damping is the worst case: force measurements show force overshoots and unstable behaviours in the first phases of the assembly task and the task fails during the third phase (the manipulated shape escapes from the desired mounting location). Common industrial robots are characterized by high stiffness and low damping parameters, so this configuration is very interesting for industrial applications.

Interaction forces in direction X and Y present the same behaviour shown in Figure 3.

In Figure 4 stiffness $\mathbf{K}$ and damping $\mathbf{D}$ parameters in direction Z of the impedance shaping control are shown. Stiffness and damping parameters adapt them self based on interaction forces.

5 CONCLUSIONS

In this paper the impedance shaping control strategy has been described and tested in a full rigid body assembly real task with compliant support. The method is capable to avoid force overshoots while allowing to track a force reference using an estimate of the environment dynamic parameters. The paper shows the capability of the defined control strategy to satisfy the desired requirements and compares the obtained results to constant impedance controllers, that show force overshoots and unstable behaviours.

Future work will extend the strategy to the rotational DoFs and will investigate the optimal definition of the on-line tuning functions of the stiffness and damping parameters and set-point gains. Moreover, more challenging tasks will be considered (machining and surgical tasks).

ACKNOWLEDGEMENTS

This work has been partially supported by EC FP7 ACTIVE project (FP7-ICT-2009-6-270460). Opinions or results expressed in this work are solely those of the authors and do not necessarily represent those of EC. The authors'd like to thank T. Dinon (CNR-ITIA) for expertise, setup and experimental support.

REFERENCES

Colgate, E. and Hogan, N. (1989). An analysis of contact instability in terms of passive physical equivalents. In *Robotics and Automation, 1989. Proceedings., 1989 IEEE International Conference on*, pages 404–409.

Dubey, R. V., Chan, T. F., and Everett, S. E. (1997). Variable damping impedance control of a bilateral telerobotic system. *Control Systems, IEEE*, 17(1):37–45.

Ferraguti, F., Secchi, C., and Fantuzzi, C. (2013). A tank-based approach to impedance control with variable stiffness. In *Proceedings of the 2013 International Conference on Robotics and Automation (ICRA)*.

Flügge, W. (1975). *Viscoelasticity*. Springer New York.

Hogan, N. (1984). Impedance control: An approach to manipulation. In *American Control Conference, 1984*, pages 304–313.

Ikeura, R. and Inooka, H. (1995). Variable impedance control of a robot for cooperation with a human. In *Robotics and Automation, 1995. Proceedings., 1995 IEEE International Conference on*, volume 3, pages 3097–3102. IEEE.

Khatib, O. (1987). A unified approach for motion and force control of robot manipulators: The operational space formulation. *Robotics and Automation, IEEE Journal of*, 3(1):43–53.

Lee, K. and Buss, M. (2000). Force tracking impedance control with variable target stiffness. *The Intern. Federation of Automatic Control*, 16(1):6751–6756.

Mason, M. T. (1981). Compliance and force control for computer controlled manipulators. *Systems, Man and Cybernetics, IEEE Transactions on*, 11(6):418–432.

Park, J. H. and Cho, H. C. (1998). Impedance control with varying stiffness for parallel-link manipulators. In *American Control Conference, 1998. Proceedings of the 1998*, volume 1, pages 478–482. IEEE.

Raibert, M. and Craig, J. (1981). Hybrid position/force control of manipulators. *Journal of Dynamic Systems, Measurement, and Control*, 103(2):126–133.

Roveda, L., Vicentini, F., and Tosatti, L. M. (2013). Deformation-tracking impedance control in interaction with uncertain environments. In *Intelligent Robots and Systems (IROS), 2013 IEEE/RSJ International Conference*, pages 1992–1997. IEEE.

Salisbury, J. K. (1980). Active stiffness control of a manipulator in cartesian coordinates. In *Decision and Control including the Symposium on Adaptive Processes, 1980 19th IEEE Conference on*, volume 19, pages 95–100.

Seraji, H. and Colbaugh, R. (1997). Force tracking in impedance control. *The International Journal of Robotics Research*, 16(1):97–117.

Villani, L., Canudas de Wit, C., and Brogliato, B. (1999). An exponentially stable adaptive control for force and position tracking of robot manipulators. *Automatic Control, IEEE Transactions on*, 44(4):798–802.

Volpe, R. and Khosla, P. (1995). The equivalence of second-order impedance control and proportional gain explicit force control. *The International journal of robotics research*, 14(6):574–589.

Yang, C., Ganesh, G., Haddadin, S., Parusel, S., Albu-Schaeffer, A., and Burdet, E. (2011). Human-like adaptation of force and impedance in stable and unstable interactions. *Robotics, IEEE Transactions on*, 27(5):918–930.

Yoshikawa, T. (1987). Dynamic hybrid position/force control of robot manipulators–description of hand constraints and calculation of joint driving force. *Robotics and Automation, IEEE Journal of*, 3(5):386–392.

Yoshikawa, T. and Sudou, A. (1990). Dynamic hybrid position/force control of robot manipulators: On-line estimation of unknown constraint. In Hayward, V. and Khatib, O., editors, *Experimental Robotics I*, volume 139 of *Lecture Notes in Control and Information Sciences*, pages 116–134. Springer Berlin Heidelberg.